PAPER

Effect of activated carbon electrode material characteristics on hardness control performance of membrane capacitive deionization†

Hongsik Yoon, [ID] *[a] Taijin Min,[a] Sung-Hwan Kim,[a] Gunhee Lee,[a] Dasom Oh,[b] Dong-Chan Choi[b] and Seongsoo Kim[b]

Capacitive deionization (CDI) is an electrochemical-based water treatment technology that has attracted attention as an effective hardness-control process. However, few systematic studies have reported the criteria for the selection of suitable electrode materials for membrane capacitive deionization (MCDI) to control hardness. In this study, the effect of electrode material characteristics on the MCDI performance for hardness control was quantitatively analyzed. The results showed that the deionization capacity and the deionization rate were affected by the specific capacitance and BET-specific surface area of the activated carbon electrode. In addition, the deionization rate also showed significant relationship with the BET specific surface area. Furthermore, it was observed that the deionization capacity and the deionization rate have a highly significant relationship with the BET specific surface area divided by the wettability performance expressed as the minimum wetting rate (MWR). These findings highlighted that the electrode material should have a large surface area and good wettability to increase the deionization capacity and the deionization rate of MCDI for hardness control. The results of this study are expected to provide effective criteria for selecting MCDI electrode materials aiming hardness control.

1 Introduction

Hardness in water causes serious industrial problems, such as membrane fouling, pipe clogging, and reduced heat exchange efficiency.[1,2] Therefore, various water-softening technologies have been developed to control water hardness, including chemical precipitation,[3,4] ion exchange resin processes,[5] NF/RO membrane filtration processes,[6,7] and electrodialysis processes;[8] however, each technology has its own limitations. For example, chemical precipitation and ion-exchange resin processes continuously consume chemicals.[3–5] On the other hand, NF/RO membranes and electrodialysis processes suffer from high energy requirements and membrane fouling.[9] Therefore, it is necessary to develop a safe and energy-saving water-softening technology. Capacitive deionization (CDI) has emerged as an alternative technology to address the challenges faced by conventional water-softening systems.[10] CDI treats ions in the feed water by capturing them in an electrical double layer (EDL) formed on an electrode when an electric potential is applied. As a practical example, previous studies have reported that CDI

effectively treats hardness-causing substances such as calcium and magnesium ions.[10]

However, CDI has the following two challenges that must be overcome: first, CDI suffers from the limitation of a low deionization capacity because deionization proceeds by trapping ions within the EDL on the electrode surface.[11,12] Therefore, previous studies attempted to develop electrode materials such as graphene, carbon nanotubes, metal–organic frameworks, and activated carbon with large specific surface areas.[13–18] Attempts are also being made to increase the deionization capacity by introducing electrodes that can utilize electron transfer reactions.[19–24] Second, CDI suffers from the limitation that some charge is inevitably wasted during ion adsorption, making it less energy efficient.[25,26] This is because when the EDL is formed, some charge is used to repel the equally charged ions (ions with the same potential as the electrode) present on the electrode surface from the electrode into the bulk solution, a process called "co-ion repulsion".[25,26] An effective method to control this phenomenon is to use ion-exchange membranes. Mounting a cation/anion exchange membrane in front of both electrodes reduces the charge dissipated by cation repulsion.[27] CDI systems with cation/anion exchange membranes are called membrane capacitive deionization (MCDI) systems and have recently become the most common type of CDI.[12,28]

Previous studies on MCDI have focused on optimizing operating conditions,[29–31] energy recovery,[32] and ion exchange

[a]Department of Sustainable Environment Research, Korea Institute of Machinery & Materials, Daejeon 34103, Republic of Korea

[b]EHS Research Center, Samsung Electronics Co., Ltd., Gyeonggi-do 18448, Republic of Korea

† Electronic supplementary information (ESI) available. See DOI: https://doi.org/10.1039/d3ra05615e

membrane material development.[33–35] Most importantly, research has been conducted on the development of electrode materials.[14,36–38] However, a limited number of studies focused on systematic investigation of the effect of electrode material properties on hardness deionization performance. A previous study demonstrated that a positive correlation exists between the electrochemical capacity and the deionization capacity of an electrode in a CDI system.[16] However, these studies were performed using conventional CDI systems without ion-exchange membranes. Our previous studies have systematically revealed the correlation between the characteristics of ion exchange membranes and coating agents for the deionization performance of MCDI for hardness control.[39–41] However, these studies did not investigate the effect of electrode characteristics on the hardness deionization performance of MCDI.

In this study, we aimed to quantitatively investigate the influence of electrode material characteristics on the deionization performance of MCDI for hardness control. This study aimed to provide practical criteria for the selection of MCDI electrode materials for hardness control. A total of six commercial activated carbons were selected, and their BET-specific surface area, surface resistance, contact angle, and electrochemical properties were analyzed. Furthermore, the deionization capacity, deionization rate, and energy consumption were evaluated as indicators of the MDCI's deionization performance for hardness control. Finally, an analysis of the correlation between the quantitative properties of the electrode material and the deionization performance was performed.

2 Experimental

2.1 Preparation and characterization of activated carbon electrode

Fig. 1 shows the activated carbon electrode preparation procedure, which was performed according to our previous studies.[39–42] Activated carbon, conducting agent (Ketjenblack, Mitsubishi Chemical Corp., Japan), and binder (PTFE, Sigma-Aldrich, USA) were mixed, extruded, and then dried in a vacuum oven at 120 °C for more than 12 h. The six activated carbons used in this study were as follows: MSP20X (Kansai Coke and Chemicals, Japan), CEP21 (Power Carbon Technology Co., Korea), YP50F (Kuraray Chemical Co., Japan), P60 (Kuraray Chemical Co., Japan), SX Plus (Norit, Netherlands), and S51F (Norit, Netherlands).

The specific surface area of the activated carbon was determined using BET analysis (ASAP2420, Micromeritics, USA). Activated carbon electrode analysis was performed using
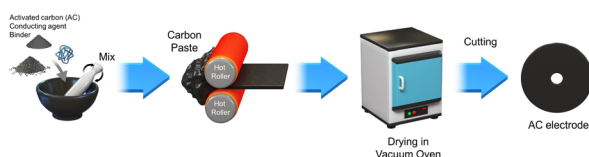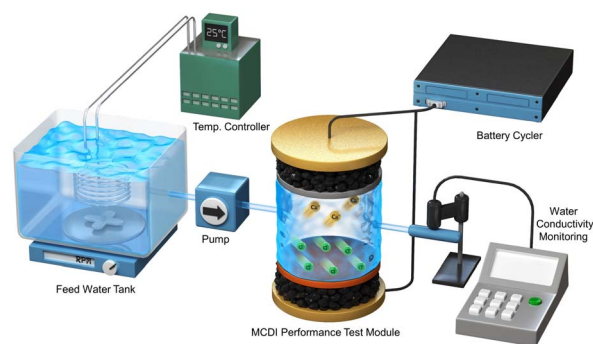

Fig. 2 Schematic of MCDI (membrane capacitive deionization) system used for evaluating deionization performance in hardness control.

surface water contact angle measurements (DSA, 100, KRUSS, Hamburg, Germany), electrode surface resistance measurements (MCP-T610, MITSUBISHI Corp., Japan), and electrochemical capacity measurements based on cyclic voltammetry (VersaSTAT3, YOUNGIN AT, Korea).

2.2 Deionization performance test

The deionization performance was evaluated using a laboratory-scale MCDI system (Fig. 2).[39–42] The MCDI system was constructed using a pair of activated carbon electrodes prepared as described in Section 2.1 and a pair of commercial cation/anion exchange membranes (Selemion CMV/AMV, AGC Engineering, Japan). All experiments were performed in the single-pass flow mode at a flow rate of 2 mL min^{-1}, where 6.25 mM of CaCl$_2$ was used as the feed solution. The adsorption and desorption were performed by applying a constant voltage of 1.2 V and -1.2 V for 10 min, respectively. Changes in ion concentration were analyzed by measuring the conductivity of the effluent (3573-10C, HORIBA, Japan). The deionization capacity, deionization rate, and energy consumption were measured according to the following eqn (1)–(3), respectively:

$$\text{Deionization capacity}\left(\text{mg g}^{-1}\right) = M_{\text{w}} \times \frac{\int (C_{\text{i}} - C_0) \times \phi \mathrm{d}t}{M_{\text{e}}} \quad (1)$$

$$\text{Deionization rate}\left(\text{mg g}^{-1}\text{ s}^{-1}\right) = M_{\text{w}} \times \frac{\int (C_{\text{i}} - C_0) \times \phi \mathrm{d}t}{M_{\text{e}} \times t} \quad (2)$$

$$\text{Energy consumption}\left(\text{W h per g-CaCl}_2\right) = \frac{V \times \int I \mathrm{d}t}{\int (C_{\text{i}} - C_0) \times \phi \mathrm{d}t} \quad (3)$$

where, M_{w} is the molecular weight of CaCl$_2$ (111 g mol^{-1}), C_{i} and C_0 are the ionic concentrations of the influent and effluent, respectively (mM), Φ is the flow rate (mL min^{-1}), t is the time (min), M_{e} is the electrode weight (g), F is Faraday's constant (96 485 C mol^{-1}), and I is the current (A).

3 Results and discussion

3.1 Characteristics of activated carbon electrodes

The water contact angle, surface resistivity, specific capacitance the BET-specific surface area were evaluated as indicators of the

Fig. 1 Schematics of the sequential preparation of activated carbon (AC) electrodes.
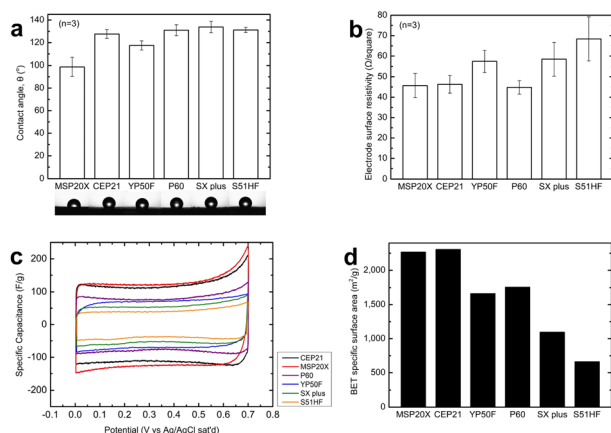
Fig. 3 Characteristics of the activated carbon electrode materials expressed as (a) contact angle, (b) electrode surface resistivity, (c) specific capacitance, and (d) BET-specific surface area.

material characteristics, as shown in Fig. 3. From Fig. 3(a), the water contact angle was found to be distributed from $98.7 \pm 8.3°$ to $133.8 \pm 8.3°$. All activated carbons had water contact angles greater than 90°, implying that they were all hydrophobic. Among the six activated carbon electrodes, MSP20X exhibited a water contact angle of 98.7°, which was significantly lower than that of the other activated carbon electrodes (117.5–133.8°). In other words, the surface of MSP20X was more hydrophilic than that of other activated carbon electrodes, which could have a positive effect on its deionization performance.[20,22,23,43,44] Fig. 3(c) shows the surface resistance in the range of 44.8 ± 3.3 to 68.4 ± 10.8 Ω per square. P60 exhibited the lowest surface resistivity within the error bars. Fig. 3(d) shows the specific capacitance, which is an indicator of the electrochemical capacity of the electrodes and was evaluated in calcium solution (1 M $CaCl_2$). From Fig. 3(d), a rectangular cyclic voltammetric profile for all the activated carbons can be observed, which is typical for capacitor-type electrodes. This indicates that no electron transfer reactions occur within the typical potential range of capacitor-type electrodes.[20,22,23] Analyzing the results in Fig. 3(c), no electron transfer reactions occurred within the corresponding potential range (0–0.7 V vs. Ag/AgCl). Quantitatively, the capacitances of the electrodes ranged from 44 to 122 F g^{-1}. MSP20X had the highest capacitance at 122 F g^{-1}, followed by CEP21, P60, YP50F, SX Plus, and S51HF at 120, 74, 71, 63, and 44 F g^{-1}, respectively. Fig. 3(d) shows the BET-specific surface area of activated carbon powder, which varied from 660 to 2305 m² g^{-1}. As shown in Fig. 3(d), CEP21 and MSP20X have the highest BET-specific surface areas at 2305 and 2266 m² g^{-1}, respectively, followed by P60, YP50F, SX Plus, and S51HF at 1765, 1662, 1096, and 660 m² g^{-1}, respectively.

3.2 MCDI deionization performance for hardness control

Fig. 4(a) and (b) shows the deionization performance of MCDI for hardness control with six activated carbon electrodes, representing the deionization capacity, deionization rate, and
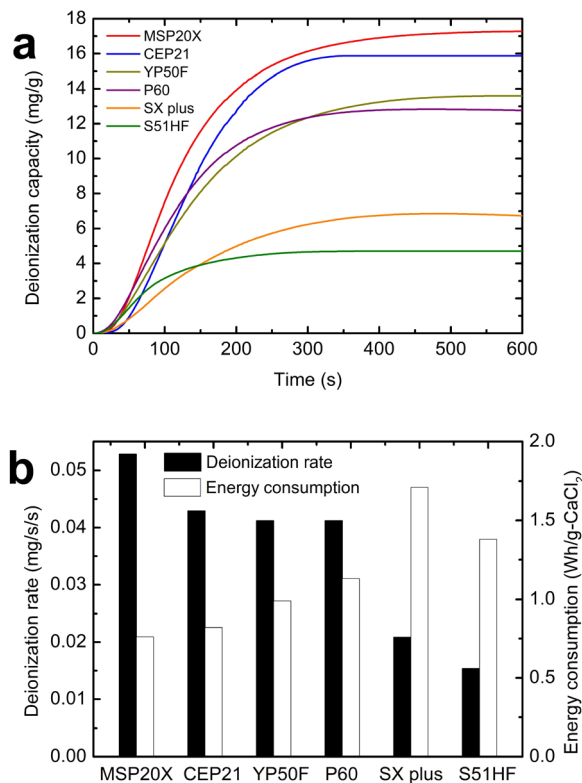

Fig. 4 MCDI's deionization performance for the hardness control with the commercial activated carbon electrode, expressed in terms of (a) deionization capacity, (b) deionization rate and energy consumption. Representative results were shown from the triplicate experiment. (Flow rate: 2 mL min^{-1}, feed: 6.25 mM $CaCl_2$, and temp.: 25 °C).

energy consumption, respectively (eqn (1)–(3)). Representative experimental results were provided from the triplicate experiments. Fig. 4(a) shows the deionization capacity, which was distributed from 4.7 to 17.3 mg g^{-1} at the maximum deionization capacity. The activated carbon electrode that achieved the highest maximum deionization capacity was MSP20X with 17.3 mg g^{-1}, followed by CEP21, YP50F, P60, SX Plus, and S51HF with deionization capacities of 16.9, 13.6, 12.8, 6.9, and 4.7 mg g^{-1}, respectively. In Fig. 4(b), the deionization rates were shown, ranging from 0.015 to 0.053 mg g^{-1} s^{-1}. For a fair comparison, the deionization rates measured over the same time period (300 s) were compared. The activated carbon electrode that achieved the highest maximum deionization rate was MSP20X with 0.053 mg g^{-1} s^{-1}, followed by CEP21, P60, YP50F, SX Plus, and S51HF with maximum deionization rates of 0.043, 0.041, 0.041, 0.021, and 0.015 mg g^{-1} s^{-1}, respectively. In addition, in Fig. 4(b), the MCDI's energy consumption was shown based on eqn (3). From the energy consumption in Fig. 4(b), the energy consumption ranged from 0.76 to 1.71 W h per g-$CaCl_2$, in the order of MSP20X < CEP21 < YP50F < P60 < S51HF < SX Plus.

Since conventional MCDI is a system based on a typical capacitor-type electrode, the deionization performance (deionization capacity, deionization rate, and energy consumption) depends on the applied potential, current, and ion

concentration of the feed water. Therefore, the deionization performance observed in Fig. 4 is limited to representing the inherent performance of the electrode and can only be used for a relative comparison.

3.3 Correlation between electrode material characteristics and MCDI deionization performance

Fig. 5(a)–(h) show the first-order plots of the deionization capacity and deionization rate as a function of the characteristics of the activated carbon electrode. Fig. 5(a) and (b) shows the deionization capacity and the deionization rate with respect to the specific capacitance. As shown in Fig. 5(a) a significant relationship is observed between the deionization capacity and the specific capacitance, with $R^2 = 0.79$. The relationship between the specific capacitance of the electrode and deionization capacity has been reported in previous studies.[16] According to the previous study, the CDI system is based on a capacitor system; therefore, the electrochemical capacity

based on the capacitance of the electrode can directly affect the deionization capacity.[16] However, the capacitance of the electrode can vary depending on the concentration of the electrolyte and the scan rate during the measurement. Therefore, the capacitance of the electrode has limited versatility for practical applications. Fig. 5(c) and (d) show that the deionization capacity and the deionization rate are also significantly correlated to the BET-specific surface area value with $R^2 = 0.96$ and 0.90, respectively. The larger the specific surface area of the electrode, the greater is the formation of the EDL, which is expected to have a positive effect on the deionization capacity. This is because deionization in MCDI is achieved by removing ions from the feed water and storing them in the double layer of the electrode. Therefore, the relationship between the BET-specific surface area and the deionization capacity appears to be plausible.

However, a comparison of BET-specific surface areas of activated carbon is insufficient to predict the deionization capacity and the deionization rate, as contradictory relationships are observed in Fig. 5(c) and (d). For example, in Fig. 5(c) and (d), MSP20X has a lower BET specific surface area than that of CEP21 but a higher deionization capacity and deionization rate. Furthermore, in Fig. 5(c), YP50F has a lower BET-specific surface area than that of P60 but a higher deionization capacity. Consequently, it can be assumed that other characteristics besides the BET-specific surface area affect deionization performance. Therefore, by adding other material properties to the BET-specific surface area, the relationship between the characteristics of the electrode materials and the MCDI performance for hardness control can be improved.

Fig. 5(e)–(h) show the deionization capacity and the deionization rate with respect to the contact angle and surface resistivity of the activated carbon electrode, respectively. As shown in Fig. 5(e)–(h), no significant correlation was observed; however, this result does not indicate that the contact angle and surface resistivity have no effect on the deionization capacity. It is speculated that the deionization capacity and deionization rate are more strongly influenced by other factors such as specific surface area. The contact angle and surface resistivity may have secondary effect on the deionization capacity and deionization rate. For example, the wettability of the electrode, which was qualitatively evaluated by the contact angle, is known to influence the MCDI performance.[43] Many previous studies have reported that electrodes with highly wettable surfaces have a positive effect on deionization performance.[20,22,23,43,44]

On the other hand, no clear relationship was observed between the characteristics of the activated carbon electrode and the energy consumption (refer to Fig. S1 in ESI†). However, it cannot be conclusively stated that no correlation exists between the properties of the activated carbon electrode and the energy consumption. This is because the deionization performance can be affected by the operating conditions such as the flow rate, ion concentration of the feed water, and applied voltage. However, in this study, only deionization capacity and deionization rate were selected and analyzed as the main performance indicator.
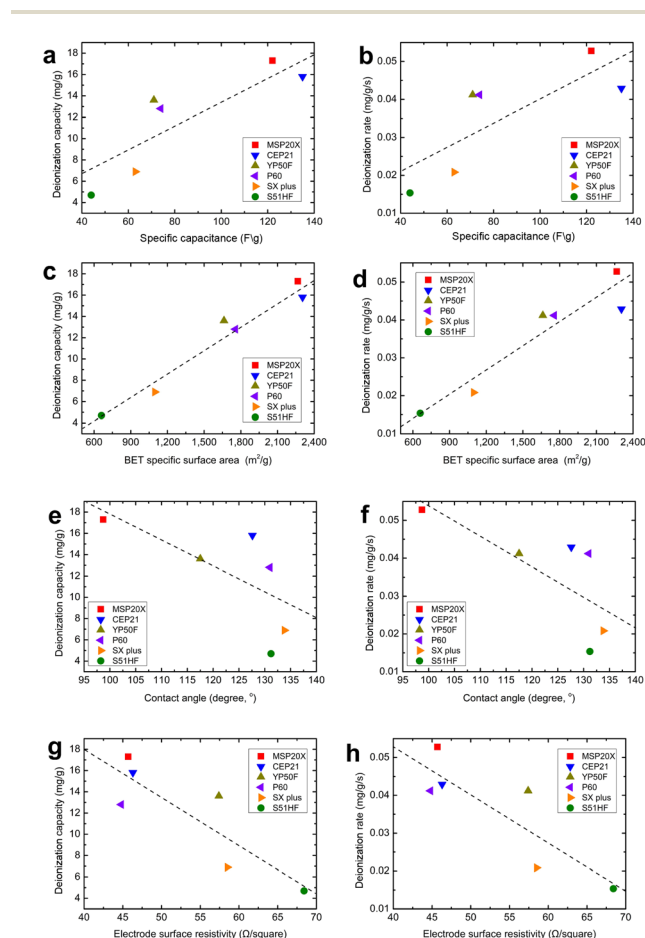

Fig. 5 Deionization capacity and deionization rate of MCDI for hardness control with respect to (a and b) specific capacitance, (c and d) BET-specific surface area, (e and f) contact angle, and (g and h) surface resistivity. The dashed line represents the trend line. Representative experimental results were provided from the triplicate experiments. The error range was within 10%. (Flow rate: 2 mL min^{-1}, feed: 6.25 mM CaCl$_2$, and temp.: 25 °C).

3.4 New characteristic indicator: BET specific surface area (σ_{BET})/minimum wetting rate (Γ_{min})

As a quantitative expression of wettability, the minimum wetting rate (MWR) has been used as a wettability performance metric.[45–48] The physical meaning of MWR is the minimum flow rate required to completely wet a surface; a lower MWR indicates better wetting performance. This MWR-contact angle relationship, which is based on the minimum total energy, has been reported in previous literature to correlate well with experimental values.[45] The MWR can be obtained from the contact angle measurement by the eqn (4) and (5), which are listed in Table 1. As shown in Table 1, the contact angles of the activated carbon electrodes used in this study ranged from 98.7° to 133.8°, and the corresponding MWRs ranged from 1.08 to 1.71. Quantitatively, the MWR of SX Plus, which has the largest contact angle, was approximately 58% higher than that of MSP20X, which had the lowest contact angle. From the MWR values, it was possible to quantify the impact of the electrode wettability.

$$\Gamma_{min} = 0.67(\Delta_{min})^{2.83} + 0.26(\Delta_{min})^{9.51} \quad (4)$$

$$\Delta_{min} = (1 - \cos\theta)^{0.22} \quad (5)$$

Γ_{min} is MWR, Δ_{min} is minimum liquid film thickness, and θ is the water contact angle (°).

Fig. 6(a) and (b) shows the relationship between the BET-specific surface area (σ_{BET}) of the activated carbon and the wettability performance metrics (*i.e.*, MWR, Γ_{min}) in combination with the deionization capacity and the deionization rate. As shown in Fig. 6(a), the relationship between $\ln(\sigma_{BET}/\Gamma_{min})$ and the deionization capacity is almost linear at $R^2 = 0.97$. Additionally, in Fig. 6(b), the relationship between $\ln(\sigma_{BET}/\Gamma_{min})$ and the deionization rate is also almost linear at $R^2 = 0.96$. The physical meaning of $\ln(\sigma_{BET}/\Gamma_{min})$ is as follows: a higher value means that the activated carbon electrode has a larger specific surface area relative to its wetting performance, and conversely, a lower value means that the electrode has a smaller specific surface area relative to its wetting performance. The results in Fig. 6 show an improved relationship compared to those in Fig. 5(c) and (d). For example, in Fig. 5(c), a contradictory relationship between the BET-specific surface area and deionization capacity can be observed for MSP20X and CEP21, and P60 and YP50F. However, the $\ln(\sigma_{BET}/\Gamma_{min})$ presented in Fig. 6
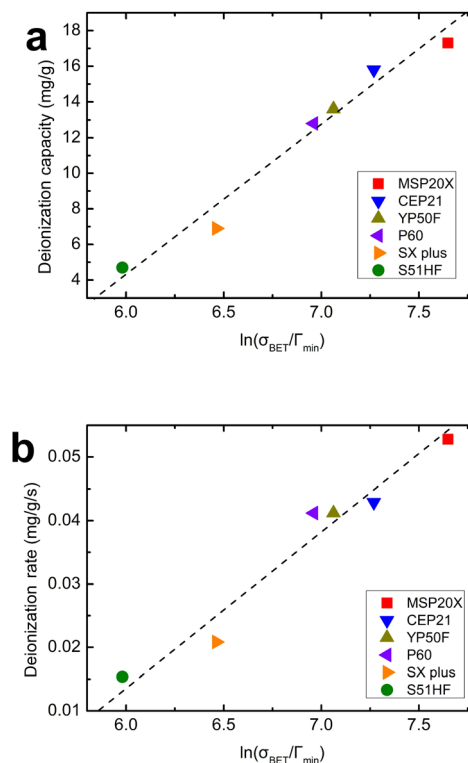

Fig. 6 (a) Deionization capacity and (b) deionization rate of membrane capacitive deionization (MCDI) for hardness control with respect to $\ln(\sigma_{BET}/\Gamma_{min})$. ($\sigma_{BET}$: BET specific surface area, Γ_{min}: minimum wetting rate (MWR)). The dashed line represents the trend line; (a) $R^2 = 0.97$ and (b) $R^2 = 0.96$. Representative experimental results were provided from the triplicate experiments. The error range was within 10%. (Flow rate: 2 mL min^{-1}, feed: 6.25 mM CaCl$_2$, and temp.: 25 °C).

resolved the contradictory relationship observed in Fig. 5(c) and (d). This improved result is likely attributed to the simultaneous consideration of the BET-specific surface area and wettability performance of the electrode. To the best of our knowledge, this is the first report to introduce a new characteristic indicator that considers specific surface area and wettability performance together. The results in Fig. 6 suggest that not only the BET-specific surface area but also the wettability performance should be considered as properties of the electrode material that can affect the deionization performance.

4 Conclusions

In this study, the impact of electrode material properties on the performance of MCDI for hardness control was quantitatively analyzed. The results showed that the deionization capacity is significantly related to the specific capacitance of the electrode. In addition, the deionization capacity and the deionization rate showed the significant relationship with the BET surface area (σ_{BET}) of the activated carbon. This study went one step further and introduced an important new characteristic indicator, $\sigma_{BET}/\Gamma_{min}$ (minimum wetting rate, MWR), which is the ratio of the BET specific surface area to the wettability performance. The analysis showed that the deionization capacity and the

Table 1 Wettability performance expressed as minimum wetting rate (MWR, Γ_{min}) with the activated carbon electrode

Activated carbon electrode	Contact angle (°) ($n = 3$)	Γ_{min}
MSP20X	98.7 ± 8.3	1.08 ± 0.15
CEP21	127.6 ± 4.0	1.61 ± 0.07
YP50F	117.5 ± 4.1	1.42 ± 0.07
P60	131.0 ± 4.9	1.66 ± 0.08
SX Plus	133.8 ± 5.1	1.71 ± 0.08
S51HF	131.2 ± 2.3	1.67 ± 0.04

deionization rate have a highly significant positive relationship with $\ln(\sigma_{BET}/\Gamma_{min})$ ($R^2 = 0.97$ and 0.96, respectively). Consequently, the electrode material should have both a high specific surface area and good wettability to increase the MCDI deionization capacity and the rate. The results of this study are expected to provide effective criteria for selecting electrode materials for hardness control in MCDIs.

Author contributions

Hongsik Yoon designed and performed the experiments and wrote the manuscript. Taijin Min, Sung-Hwan Kim, Gunhee Lee, Dasom Oh, Dong-Chan Choi, Seongsoo Kim contributed to revising the manuscript.

Conflicts of interest

There are no conflicts to declare.

Acknowledgements

References

1 C. Gabrielli, G. Maurin, H. Francy-Chausson, P. Thery, T. Tran and M. Tlili, Electrochemical water softening: principle and application, *Desalination*, 2006, **201**, 150–163.

2 J.-S. Park, J.-H. Song, K.-H. Yeon and S.-H. Moon, Removal of hardness ions from tap water using electromembrane processes, *Desalination*, 2007, **202**, 1–8.

3 J. G. Dean, F. L. Bosqui and K. H. Lanouette, Removing heavy metals from waste water, *Environ. Sci. Technol.*, 1972, **6**, 518–522.

4 M. Nagarajan and H. Paine, Water hardness control by detergent builders, *J. Am. Oil Chem. Soc.*, 1984, **61**, 1475–1478.

5 B. H. Wiers, R. J. Grosse and W. A. Cilley, Divalent and trivalent ion exchange with zeolite A, *Environ. Sci. Technol.*, 1982, **16**, 617–624.

6 S. Ghizellaoui, A. Chibani and S. Ghizellaoui, Use of nanofiltration for partial softening of very hard water, *Desalination*, 2005, **179**, 315–322.

7 A. R. Hauck and S. Sourirajan, Performance of porous cellulose acetate membranes for the reverse osmosis treatment of hard and waste waters, *Environ. Sci. Technol.*, 1969, **3**, 1269–1275.

8 K.-H. Yeon, J.-H. Song and S.-H. Moon, A study on stack configuration of continuous electrodeionization for removal of heavy metal ions from the primary coolant of a nuclear power plant, *Water Res.*, 2004, **38**, 1911–1921.

9 J.-H. Song, K.-H. Yeon, J. Cho and S.-H. Moon, Effects of the operating parameters on the reverse osmosis-electrodeionization performance in the production of high purity water, *Korean J. Chem. Eng.*, 2005, **22**, 108–114.

10 S.-J. Seo, H. Jeon, J. K. Lee, G.-Y. Kim, D. Park, H. Nojima, J. Lee and S.-H. Moon, Investigation on removal of hardness ions by capacitive deionization (CDI) for water softening applications, *Water Res.*, 2010, **44**, 2267–2275.

11 S. Kumar, N. M. Aldaqqa, E. Alhseinat and D. Shetty, Electrode materials for desalination of water via capacitive deionization, *Angew. Chem., Int. Ed.*, 2023, e202302180.

12 P. Biesheuvel and A. Van der Wal, Membrane capacitive deionization, *J. Membr. Sci.*, 2010, **346**, 256–262.

13 H. Qiang, M. Shi, F. Wang and M. Xia, Green synthesis of high N-doped hierarchical porous carbon nanogranules with ultra-high specific surface area and porosity for capacitive deionization, *Sep. Purif. Technol.*, 2023, **308**, 122918.

14 Y. Zhang, X. Bu, Y. Wang, Z. Hang and Z. Chen, Hierarchically porous biochar derived from aerobic granular sludge for high-performance membrane capacitive deionization, *Environ. Sci. Ecotechnology*, 2023, 100297.

15 H. Zhang, J. Tian, X. Cui, J. Li and Z. Zhu, Highly mesoporous carbon nanofiber electrodes with ultrahigh specific surface area for efficient capacitive deionization, *Carbon*, 2023, **201**, 920–929.

16 T. Kim and J. Yoon, Relationship between capacitance of activated carbon composite electrodes measured at a low electrolyte concentration and their desalination performance in capacitive deionization, *J. Electroanal. Chem.*, 2013, **704**, 169–174.

17 Y. Wimalasiri and L. Zou, Carbon nanotube/graphene composite for enhanced capacitive deionization performance, *Carbon*, 2013, **59**, 464–471.

18 R. T. Mayes, C. Tsouris, J. O. Kiggans Jr, S. M. Mahurin, D. W. DePaoli and S. Dai, Hierarchical ordered mesoporous carbon from phloroglucinol-glyoxal and its application in capacitive deionization of brackish water, *J. Mater. Chem.*, 2010, **20**, 8674–8678.

19 S. Wang, G. Wang, C. He, N. Gao, B. Lu, L. Zhao, J. Weng, S. Zeng and C. Li, Enabling superior hybrid capacitive deionization performance in NASICON-structured Na 3 MnTi (PO 4) 3/C by incorporating a two-species redox reaction, *J. Mater. Chem. A*, 2021, **9**, 6898–6904.

20 H. Yoon, J. Lee, T. Min, G. Lee and M. Oh, High performance hybrid capacitive deionization with a Ag-coated activated carbon electrode, *Environ. Sci.: Water Res. Technol.*, 2021, **7**, 1315–1321.

21 J. Lee, S. Kim, C. Kim and J. Yoon, Hybrid capacitive deionization to enhance the desalination performance of capacitive techniques, *Energy Environ. Sci.*, 2014, **7**, 3683–3689.

22 H. Yoon, J. Lee, S. Kim and J. Yoon, Hybrid capacitive deionization with Ag coated carbon composite electrode, *Desalination*, 2017, **422**, 42–48.

23 H. Yoon, T. Min, J. Lee, G. Lee, M. Jeon and A. Kim, Lithium-selective hybrid capacitive deionization system with a Ag-coated carbon electrode and stop-flow operation, *Environ. Sci.: Water Res. Technol.*, 2023, **9**, 500–507.

24 S. Kim, J. Lee, C. Kim and J. Yoon, Na2FeP2O7 as a novel material for hybrid capacitive deionization, *Electrochim. Acta*, 2016, **203**, 265–271.

25 T. Kim, J. Dykstra, S. Porada, A. Van Der Wal, J. Yoon and P. Biesheuvel, Enhanced charge efficiency and reduced energy use in capacitive deionization by increasing the discharge voltage, *J. Colloid Interface Sci.*, 2015, **446**, 317–326.

26 E. Avraham, Y. Bouhadana, A. Soffer and D. Aurbach, Limitation of Charge efficiency in capacitive deionization: I. On the behavior of single activated carbon, *J. Electrochem. Soc.*, 2009, **156**, P95.

27 J.-B. Lee, K.-K. Park, H.-M. Eum and C.-W. Lee, Desalination of a thermal power plant wastewater by membrane capacitive deionization, *Desalination*, 2006, **196**, 125–134.

28 M. D. Andelman and G. S. Walker, Charge barrier flow-through capacitor-based method of deionizing a fluid, *US Pat.*, US8002963B2, 2011.

29 R. Zhao, P. Biesheuvel and A. Van der Wal, Energy consumption and constant current operation in membrane capacitive deionization, *Energy Environ. Sci.*, 2012, **5**, 9520–9527.

30 E. Garcia-Quismondo, C. Santos, J. Lado, J. Palma and M. A. Anderson, Optimizing the energy efficiency of capacitive deionization reactors working under real-world conditions, *Environ. Sci. Technol.*, 2013, **47**, 11866–11872.

31 J.-H. Lee and J.-H. Choi, The production of ultrapure water by membrane capacitive deionization (MCDI) technology, *J. Membr. Sci.*, 2012, **409**, 251–256.

32 P. Długołecki and A. van der Wal, Energy recovery in membrane capacitive deionization, *Environ. Sci. Technol.*, 2013, **47**, 4904–4910.

33 G. Tian, L. Liu, Q. Meng and B. Cao, Preparation and characterization of cross-linked quaternised polyvinyl alcohol membrane/activated carbon composite electrode for membrane capacitive deionization, *Desalination*, 2014, **354**, 107–115.

34 N.-S. Kwak, J. S. Koo, T. S. Hwang and E. M. Choi, Synthesis and electrical properties of NaSS–MAA–MMA cation exchange membranes for membrane capacitive deionization (MCDI), *Desalination*, 2012, **285**, 138–146.

35 J. S. Koo, N.-S. Kwak and T. S. Hwang, Synthesis and properties of an anion-exchange membrane based on vinylbenzyl chloride–styrene–ethyl methacrylate copolymers, *J. Membr. Sci.*, 2012, **423**, 293–301.

36 Y. S. Huh, M. Rethinasabapathy, G. Bhaskaran, S.-K. Hwang and T. Ryu, Efficient Lithium Extraction Using Redox-Active Prussian Blue Nanoparticles-Anchored Activated Carbon Intercalation Electrodes Via Membrane Capacitive Deionization, *Chemosphere*, 2023, **336**, 139256.

37 J. Chen, K. Zuo, B. Li, D. Xia, L. Lin, J. Liang and X.-y. Li, Embedment of graphene in binder-free fungal hypha-based electrodes for enhanced membrane capacitive deionization, *Sep. Purif. Technol.*, 2023, **304**, 122381.

38 H. Yu, S. M. Hossain, C. Wang, Y. Choo, G. Naidu, D. S. Han and H. K. Shon, Selective lithium extraction from diluted binary solutions using metal-organic frameworks (MOF)-based membrane capacitive deionization (MCDI), *Desalination*, 2023, **556**, 116569.

39 H. Yoon, T. Min, G. Lee, I. Park, B. Han, S. K. Bo, K. Ryu and J. Lee, Development of capacitive deionization with calcium alginate based cation exchange membrane for hardness control, *Journal of the Korean Society of Industry Convergence*, 2021, **24**, 563–571.

40 H. Yoon, J. Lee, S.-R. Kim, J. Kang, S. Kim, C. Kim and J. Yoon, Capacitive deionization with Ca-alginate coated-carbon electrode for hardness control, *Desalination*, 2016, **392**, 46–53.

41 H. Yoon, K. Jo, K. J. Kim and J. Yoon, Effects of characteristics of cation exchange membrane on desalination performance of membrane capacitive deionization, *Desalination*, 2019, **458**, 116–121.

42 H. Yoon, T. Min, G. Lee, M. Jeon, M. Oh and A. Kim, Hybrid Capacitive Deionization with Ag-coated Activated Carbon Electrodes for Nickel Treatment, *Environ. Eng. Res.*, 2023, **28**, 220657.

43 K. Jo, Y. Baek, C. Lee and J. Yoon, Effect of Hydrophilicity of Activated Carbon Electrodes on Desalination Performance in Membrane Capacitive Deionization, *Appl. Sci.*, 2019, **9**, 5055.

44 C. Kim, J. Lee, S. Kim and J. Yoon, TiO2 sol–gel spray method for carbon electrode fabrication to enhance desalination efficiency of capacitive deionization, *Desalination*, 2014, **342**, 70–74.

45 A. Martinez-Urrutia, P. F. de Arroiabe, M. Ramirez, M. Martinez-Agirre and M. M. Bou-Ali, Contact angle measurement for LiBr aqueous solutions on different surface materials used in absorption systems, *Int. J. Refrig.*, 2018, **95**, 182–188.

46 A. Doniec, Laminar flow of a liquid rivulet down a vertical solid surface, *Can. J. Chem. Eng.*, 1991, **69**, 198–202.

47 M. S. El-Genk and H. H. Saber, Minimum thickness of a flowing down liquid film on a vertical surface, *Int. J. Heat Mass Transfer*, 2001, **44**, 2809–2825.

48 A. B. Ponter, G. A. Davies, T. K. Ross and P. G. Thornley, The influence of mass transfer on liquid film breakdown, *Int. J. Heat Mass Transfer*, 1967, **10**, 349–352.